Nanotechnology **20** (2009) 255101 (8pp) doi:10.1088/0957-4484/20/25/255101

Toxicity induced enhanced extracellular matrix production in osteoblastic cells cultured on single-walled carbon nanotube networks

Wojtek Tutak[1], Ki Ho Park[2], Anatoly Vasilov[2], Valentin Starovoytov[3], Giovanni Fanchini[1], Shi-Qing Cai[2], Nicola C Partridge[2], Federico Sesti[2,4] and Manish Chhowalla[1,4]

[1] Materials Science and Engineering, School of Engineering, Rutgers, The State University of New Jersey, Piscataway, NJ 08854, USA
[2] Department of Physiology and Biophysics, The University of Medicine and Dentistry of New Jersey—Robert Wood Johnson Medical School, Piscataway, NJ 08854, USA
[3] Department of Cell Biology and Neuroscience, Rutgers, The State University of New Jersey, Piscataway, NJ 08855, USA

E-mail: sestife@umdnj.edu and manish1@rci.rutgers.edu

Received 25 February 2009, in final form 1 May 2009
Published 2 June 2009
Online at stacks.iop.org/Nano/20/255101

Abstract
A central effort in biomedical research concerns the development of materials for sustaining and controlling cell growth. Carbon nanotube based substrates have been shown to support the growth of different kinds of cells (Hu *et al* 2004 *Nano Lett.* **4** 507–11; Kalbacova *et al* 2006 *Phys. Status Solidi* b **13** 243; Zanello *et al* 2006 *Nano Lett.* **6** 562–7); however the underlying molecular mechanisms remain poorly defined. To address the fundamental question of mechanisms by which nanotubes promote bone mitosis and histogenesis, primary calvariae osteoblastic cells were grown on single-walled carbon nanotube thin film (SWNT) substrates. Using a combination of biochemical and optical techniques we demonstrate here that SWNT networks promote cell development through two distinct steps. Initially, SWNTs are absorbed in a process that resembles endocytosis, inducing acute toxicity. Nanotube-mediated cell destruction, however, induces a release of endogenous factors that act to boost the activity of the surviving cells by stimulating the synthesis of extracellular matrix.

(Some figures in this article are in colour only in the electronic version)

1. Introduction

A major effort in bone bioengineering research is to design new materials to support, increase and/or replace bone tissue. In recent years, several materials [4–6], as well as distinct original processing techniques [7–9], have been proposed and tested. Among them, single-walled carbon nanotubes (SWNTs) have raised considerable interest because these materials possess unique mechanical, thermal and electrical properties [10–12]. Despite an intense effort, however, the notion that carbon nanotubes can have practical biomedical applications remains controversial [13]. While several studies have reported that a variety of cell lines of different species can grow on carbon nanotube substrates [1, 2, 14], others have underscored a significant level of toxicity intrinsic to these nanomaterials [15, 16]. Moreover, many issues such as long-term effects, whether carbon nanotubes can support the growth of primary cells and, more importantly, what are the mechanisms by which they act to stimulate multiple cellular activities remain to be elucidated.

Here, we unveil a mechanism through which carbon nanotubes not only induce toxicity but also promote bone cell differentiation leading to formation of bone nodules.

[4] Authors to whom any correspondence should be addressed.

We show that SWNTs deposited onto multicellulose ester (MCE) membrane (Millipore) stimulate the production of extracellular matrix, a central step in bone tissue formation in primary rat calvariae osteoblastic cells and mouse pre-osteoblastic MC3T3-E1 cells. Intriguingly, this enhancement is related to an initial decline in cell number and increase in protein expression. This initial decrease in the cell number and increase in protein expression are further reinforced by transmission electron microscopy observations which reveal that SWNTs enter the cells within the first few hours after cell deposition. We observe that above some critical concentration and size of SWNT vacuoles within the cells (after 24 h), a decrease in total cell numbers occurs. In the absence of SWNTs entering the cells, cell toxicity is not observed. Our study suggests cell activity is strongly modulated by loose SWNTs entering the osteoblast cytoplasm.

2. Experimental details

2.1. Preparation and characterization of SWNT substrates

Raw HiPco nanotubes were purchased from 'Carbon nanotechnologies INC'. Purification procedure involved a multi-step process adopted from both Chiang *et al* and Xu *et al* and optimized in our laboratory [17–19]. Briefly, SWNTs were annealed in humid air at 230 °C for 24 h. Subsequently, SWNTs were stirred in 6 M HCl for 12 h at 70 °C followed by another humid annealing at 250 °C. Acid treatment was repeated one more time followed by an annealing step at 270 °C temperature. SWNTs were dispersed in a 1 wt.% aqueous solution of sodium dodecylsulfate (SDS) and ultrasonicated for 3 h. Typically, 8 mg of the purified nanotubes was dispersed in 1 l of 1 wt% SDS (8 μg ml^{-1}) solution. A vacuum filtration apparatus was utilized to filter the dispersed SWNT solution and uniformly deposit them onto MCE membrane with pore size of 220 nm (Millipore). The method utilized by our group was originally developed by Wu *et al* and optimized in our laboratory [20–22]. Forty milliliters of the SWNT solution was deposited on each membrane (24.6 μg/sample). Thin nanotube films deposited onto MCE membranes were cut into uniform circular samples with $d = 1.3$ or 1.2 cm covering more than 75% and 65% of a corresponding well of a 24 well culture plate ($d = 1.5$ cm) area. Smaller diameter samples were placed in a series of acetone and methanol baths and deposited on glass slides (Fisher Scientific) [21]. Pieces were then UV (254 nm) disinfected for 24 h prior to seeding. Samples were soaked for 24 h in phosphate buffer saline (PBS) solution prior to cell seeding.

2.2. Cell culture

Primary osteoblastic rat cells and the mouse MC3T3-E1 osteoblast-like cell line used in this study were grown at 37 °C in a humidified atmosphere of 5% CO_2 in air. The MC3T3-E1 cell line was supplemented with Eagle's minimal essential medium (α-MEM), 10% fetal bovine serum (FBS), 1% pen-strep bactericide (PS). MC3T3-E1 cells were seeded at 5000 cells/well. Primary calvariae cells were deposited at 16 000 cells/well for up to 28 days in 24 well Falcon tissue culture plates (Falcon® Petri dish). If not stated otherwise, the medium in both cell cultures was changed every 2–3 days and each sample type was tested in triplicates. Primary osteoblast cells were obtained from newborn rats by sequential digestion of the calvariae in a solution of Collagenase A/Trypsin followed by cell centrifugation and counting [23, 24]. The cells were then cultured in MEM containing 10% FBS, and 1% nonessential amino acids and 0.1% PS. The medium was changed every 2 or 3 days up to day 8. Thereafter, BG Jb medium supplemented with 50 μg ml^{-1} ascorbic acid and 3.06 mg ml^{-1} of β-glycerolphosphate, 10% of FBS and 1% PS was used.

2.3. Bradford total protein assays

Upon sample collection, pieces were first rinsed twice in PBS and transferred to 0.5 ml of deionized water. Cells grown directly on growth plates were removed using a standard rubber scraper. All samples were placed in a freezer for at least 24 h. Pieces were homogenized in an ultrasonic processor (Cole Parmer 750 W, model CV33) on ice for 15 s at 30% power and centrifuged at 14 000 rpm for 5 min. Assays were done according to the microprotein assay procedure [25], and normalized to a calibration curve obtained using bovine serum albumin dilutions. Twenty microliters of sample solution was mixed with 1 ml Bradford reagent in test tubes; absorbance of dye–protein complexes was measured after 1 min at 595 nm. The optical density (OD) was determined using general purpose UV/vis dual beam spectrophotometer (Beckman Coulter DU 520). Relative ratios between SWNTs on MCE or SWNTs on glass and polystyrene area were calculated and applied to normalize expressed protein values. (SWNTs on MCE/polystyrene area $1.33/1.77 = 0.75$; and SWNTs on glass/polystyrene $1.13/1.77 = 0.64$). Experiment was repeated three times.

2.4. Osteoblastic cell viability assays

Osteoblast viability and numbers were determined by testing the mitochondrial enzyme activity according to the colorimetric 3-(4,5-dimethylthiazol-2-yl)-2,5-diphenyltetrazolium bromide (Sigma Aldrich, Tox-1) assay. Accordingly, primary osteoblast cells were seeded in 24 well tissue culture plates. One hour before sample collection, pieces were very gently rinsed twice in PBS and 0.5 ml of phenol free Eagle's minimal essential media was introduced to each sample well. Upon sample collection, 50 μl of prepared MTT solution was added to each well and incubated for another 2.5 h at 37 °C. Formed formazan crystals were subsequently dissolved by adding the solubilization solution. The absorbance at 570 nm was recorded on the spectrophotometer. The optical density values were then normalized to cell number using the standard curve. The calibration curve was established using titrated cell solutions measured 24 h after cell seeding. MTT based experiments were replicated twice.

2.5. Lactate dehydrogenase (LDH) toxicity assay

Lactate dehydrogenase enzyme activity in cell supernatant was measured using the TOX-7 kit (Sigma Aldrich). SWNT on

glass, SWNT on MCE and polystyrene samples were prepared as described before. Primary osteoblastic cells were deposited at 16 000/well in serum free media, in triplicates and the test was repeated twice. Cell supernatant was collected after 2 and 24 h and processed following manufacturer procedure. Toxicity, (T) was quantified as:

$$T = \frac{A - A_{\mathrm{U}}}{A_{\mathrm{Tx}} - A_{\mathrm{U}}}$$

where the absorbances (OD) of the test sample (A), untreated cells (A_{U}) and cells lysed with Triton X-100, (A_{Tx}) were determined with a FlexStation 3 microplate reader (Molecular Devises) at 490 nm wavelength.

2.6. Alkaline phosphatase (ALP) assays

ALP activity from the scaffolds/cell samples was quantified by the specific conversion of *p*-nitrophenyl phosphate (*p*NPP) (Sigma Aldrich, P 7998) into *p*-nitrophenol (*p*NP). Samples were first rinsed twice in PBS solution and then the enzyme reaction was started by adding 1 ml of substrate buffer (*p*NPP) to samples. The solution was incubated at 37 °C for 5 min. Upon reaction completion, 200 μl of solution was withdrawn and reaction was stopped by adding 50 μl of 3 N NaOH. The OD was determined at 405 nm using the spectrophotometer. Five microliters of titrated *p*NP (Sigma Aldrich, N-7660) solutions were used to construct a standard curve and applied to convert data to absolute values (μmol h^{-1}/cell number). Data from cells grown on SWNTs on MCE were multiplied by relative area ratios as outlined before. The test was performed twice.

2.7. Biochemical assays

Cells grown on SWNT thin films and controls were washed twice with cold PBS and collected according to the method outlined above. Next, cells were lysed in 50 mM Tris-HCl (pH 6.8), 10 mM EDTA, glycerol and 10% SDS. Equal amounts of sample lysate were separated by 13% sodium dodecylsulfate polyacrylamide gel electrophoresis (SDS-PAGE) and electrophoretically transferred onto PVDF membrane (Millipore).The membrane was blocked for 2 h in 5% of commercially available dry milk and TBST solution (10 mM Tris-HCl pH 8.0, 150 mM NaCl, 0.05% Tween 20). Then, the blots were incubated with either anti-Collagen I or anti-tubulin primary antibodies (Sigma Aldrich) in the TBST solution at a 1:1000 dilution for 2 h at room temperature. Secondary anti-mouse antibodies conjugated with horseradish peroxidase at a 1:10 000 dilution were introduced and incubated for 1.5 h then visualized with an enhanced chemiluminescence (ECL) kit (*GE* Healthcare, US). Membranes were exposed to Blue Basic Autorad films (ISC Bioexpresse, US) for 5–10 min.

2.8. Cell lysates

Cell lysates for the experiments in figure 7 were obtained as follows: 30 500 ml^{-1} primary cells were dispersed in 1 ml of PBS and lysed by a series of short sonications at 160 and 266 W. A small representative sample was withdrawn and stained with trypan blue (0.04%) to verify, under the microscope, for any remaining intact cells. The remaining lysate was thoroughly mixed with 1 ml of the proliferation medium. Before any solution was added, medium was replaced in all samples. The mixture was then dispensed at 30 μl/well (4500 lysed cells/dose) to each well containing cells after 3 and 24 h. Experiment was replicated twice.

2.9. Transmission and scanning electron microscopy

The internalization of SWNTs within MC3T3-E1 osteoblasts was investigated using a TEM (JEM 100 CXII) operating at 80 kV and SEM (AMRAY-18301) using 20 kV power source. For the TEM experiments, osteoblasts cells were incubated on same number of various samples (SWNTs on glass, SWNTs on MCE and polystyrene). Specimens were collected at various times and subsequently rinsed three times in PBS and trypsinized. The samples were centrifuged for 4 min at 10 000 rpm. The resulting cell pellets were fixed in Karnovsky's Fixative for 3 h. After being washed, cells were postfixed with 1% osmium tetroxide for 1 h followed by dehydration in graded water: ethanol series (50–70–80–90–95–100%) for 10–15 min and embedded in Epon–Araldite solution. Sections were prepared using ultramicrotome. Corresponding carbon content was measured using Image J software. Black foreign bodies within cells were identified as SWNT inclusions. Average inclusion area was calculated based on six images taken for each treatment type and collection time. Samples designated for SEM analysis underwent postfixation and dehydration processes similar to that outlined for TEM. Specimens were critical point dry-processed and platinum/gold coated. This experiment was replicated two times.

2.10. Statistics

Statistical significance was assessed by the *Student t-test* and one-way ANOVA (for multiple comparisons) and corrected using post hoc ANOVA/Tukey. A 95% confidence level was considered statistically significant.

3. Results

In order to understand the cell number, differentiation and interactions of primary rat osteoblast cells on SWNT networks, we performed biochemical assays to obtain information about the total protein expression (specifically Collagen I production), cell number and alkaline phosphatase activity. Complementary to the biological measurements, we also performed scanning and transmission electron microscopy to investigate the morphology of the cell cultures and SWNT uptake as a function of time, respectively.

The purified and well dispersed SWNT networks were deposited onto a multicellulose ester membrane using the vacuum filtration method. Experimental substrates consisted of SWNTs deposited on MCE membrane (SWNTs on MCE) or well rinsed nanotubes placed on glass slides (SWNTs on glass).

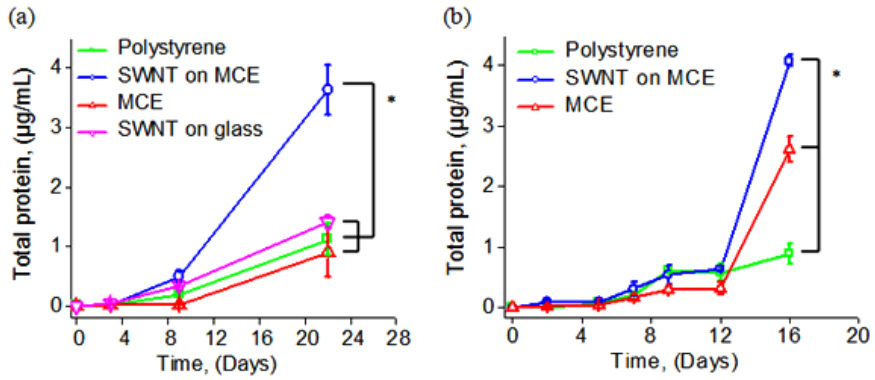

Figure 1. Total protein expression for cells grown on SWNT and control substrates. (a) Total protein content expressed in primary rat osteoblastic cells grown on SWNTs on MCE substrates (circles), rinsed SWNTs on glass samples (pointing down triangles), MCE alone (pointing up triangles) and polystyrene (squares). (b) Total protein content expressed in mouse MC3T3-E1 osteoblastic cells grown on SWNTs on MCE, MCE alone and polystyrene. Values are mean ± SD of three individual cultures. Statistically significant differences from control are indicated with ∗; $p < 0.05$.

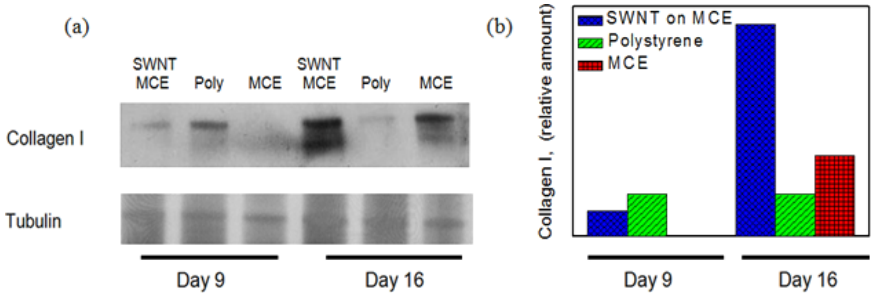

Figure 2. Increased Collagen I synthesis in cells grown on SWNTs on MCE. (a) Western visualization of Collagen I in MC3T3-E1 cells grown on the indicated substrates. Bottom, Tubulin control. (b) Densitometry analysis of Collagen I protein expression in cells cultured on SWNTs on MCE (blue bar, fine mesh) and control (polystyrene and MCE alone) at two different time points.

The SWNTs on glass adhere well after rinsing while loose SWNTs remain on the MCE membrane even after extensive washing. A negative MCE membrane and positive polystyrene control samples were incorporated into testing setup to assess and evaluate cellular response.

The total protein expression was measured by the Bradford protein assay. Results of the total protein expression comparing the controls and the SWNT networks for primary and MC3T3-E1 cell lines are shown in figures 1(a) and (b).

Both types of cells in long-term study express proteins similarly, corroborating the notion that SWNTs impact cell response in very similar ways and validating the use of a cell line (the MC3T3) that is amenable to laboratory study. More importantly, it can be clearly observed that the total protein expression in both cell lines is significantly higher for the SWNTs on MCE substrate. In contrast, the protein expression for primary cells on SWNTs on glass substrates is comparable to control.

The effect of underlying MCE membrane on the protein expression was found to be negligible as shown in figure 1(a). Thus, these results suggest that cellular activity on SWNTs on MCE is different from SWNTs on glass. The main objective of this work is to elucidate the cause of this difference.

Bone histogenesis is characterized by several distinct phases: the tissue originates from mesenchymal cells, undergoes proliferation, synthesis of extracellular matrix, mineralization of the matrix, vascular invasion, and finally death. Hence, the fact that protein expression in cells grown on SWNTs on MCE substrate increased significantly after two weeks of culture suggests that the SWNT substrates acted primarily to alter post-differentiation processes. Therefore to confirm this notion we assessed Collagen I production, a hallmark of extracellular matrix production [26], in cells seeded on SWNTs on MCE and on polystyrene for control at different time points. As shown in figure 2, Collagen I synthesis was significantly enhanced in SWNTs on MCE substrates in a time dependent fashion.

The increased protein expression and collagen production for SWNTs on MCE substrates was correlated to the cell number using the standard colorimetric 3-(4,5-dimethylthiazol-2-yl)-2,5-diphenyltetrazolium bromide assay. The cell number as a function of time for the control and SWNTs on MCE substrates is shown in figure 3(a). Significant difference between cells grown on the control and SWNTs on MCE substrate can be observed. Specifically, the number of cells increases monotonically in the control initially while it decreases (at 24 h) and then increases for the SWNTs on MCE substrate. Cell number in polystyrene samples did not substantially vary after 3 weeks at which point cells reached confluence. However, the number of cells grown on SWNTs

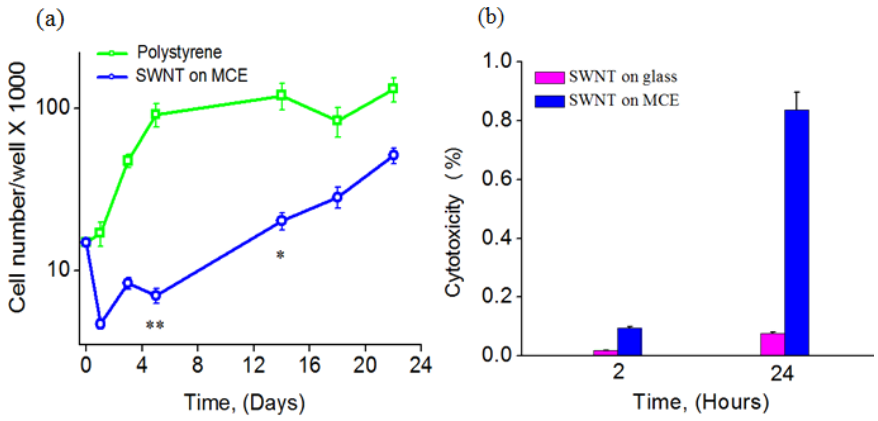

Figure 3. Primary cell viability (MTT) and lactate dehydrogenase (LDH) assays. (a) MTT colorimetric assay was applied to monitor primary osteoblastic cell viability on SWNTs on MCE and on polystyrene for control. Cell number noticeably drops within first 24 h in cell cultures grown on SWNT matrix (ovals). Values are mean ± SD of three independent cell cultures. Statistically significant differences from control are indicated with ∗; $p < 0.05$ and ∗∗; $p < 0.001$. (b) LDH levels in calvariae cells 2 and 24 h after seeding on SWNT on MCE substrate.

on MCE matrix does not fully recover to control values. The initial decrease in cell number is likely related to SWNT entry into the cells, as corroborated by our TEM investigation (see below). Nanotube toxicity was further validated using a lactase dehydrogenase (LDH) assay, figure 3(b). As expected these experiments independently confirmed the presence of ruptured cells within first 24 h after seeding.

We next measured alkaline phosphatase activity in order to obtain additional insight into the results presented in figures 1(a) and 3. These results indicate that ALP activity on SWNT films on MCE is generally enhanced in comparison to the control (figure 4). This is expected since the ALP activity reflects post-proliferation processes that are related to an increase in osteoblastic differentiation [27, 28].

The morphological characteristics of the cells were monitored by SEM as a function of time. Images taken at days 3, 17 and 23 are shown in figure 5. In contrast to the growth on control substrates, better adhesion of the primary cells was observed for SWNT networks on MCE substrates. Specifically, filopodia appendages can be seen after day 3 in figure 5(a), as indicated by the arrows. The morphology of the cells on the SWNTs on MCE substrate did not change dramatically until day 23 when nodules representing calcified tissue were clearly visible, as indicated in figure 5(c).

Based on the analysis presented above, the results appear to suggest that SWNT thin films on MCE facilitate the differentiation of osteoblastic cells leading to an increase in alkaline phosphatase activity, Collagen I production and calcification of tissue. However, our data also suggest a cytotoxic effect. In order to better understand why protein expression increases while the cell number decreases initially, detailed observation of the interactions between SWNT substrates and cells as a function of time was conducted. TEM images of the cells cultured on SWNTs on MCE for 6 and 12 h are shown in figures 6(a) and (b). Black carbonaceous inclusions of ∼0.5 μm in diameter distributed in the cell cytoplasm are clearly visible.

These dark regions increase in size and number up to 24 h, as seen in figure 6(c). At 72 h, internalized SWNTs reach a

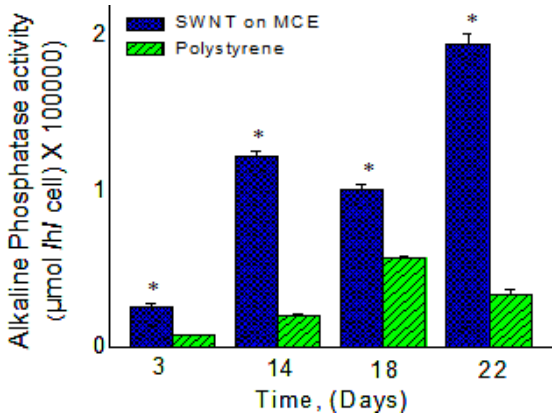

Figure 4. Alkaline phosphatase activity in primary calvariae cells cultured on the indicated substrates. Values are mean ± SD of six independent cell cultures. Statistically significant differences from control are indicated with ∗; $p < 0.05$.

diameter of ∼1 μm and appear to aggregate to form larger inclusions. TEM analysis of longer growth times (9 days, figure 6(e)) shows that the black carbon regions diminish in size, number and total area. The TEM image observations are quantified in the bar graph shown in figure 6(i). It clearly indicates that the amount of carbon nanotubes within the cells peaks at 24 h, correlating with the lowest cell count in figure 2.

This appears to suggest that critical concentration and size of SWNT clusters within the cells leads to a decrease in viable cell number. It is not surprising to observe SWNTs within the cells as recent studies have shown that biological cells can absorb carbon nanotubes via endocytosis [29]. In our case it is likely that the uptake of SWNTs occurs via release of loosely bonded nanotubes within the SWNT network deposited on top of MCE membrane. Once cells are seeded onto SWNTs on MCE substrate, they interact with nanotubes and likely enter the cells via phagocytosis [30]. It should be mentioned that no such exogenous clusters were observed within cells grown on polystyrene substrates as depicted in figure 6(f).

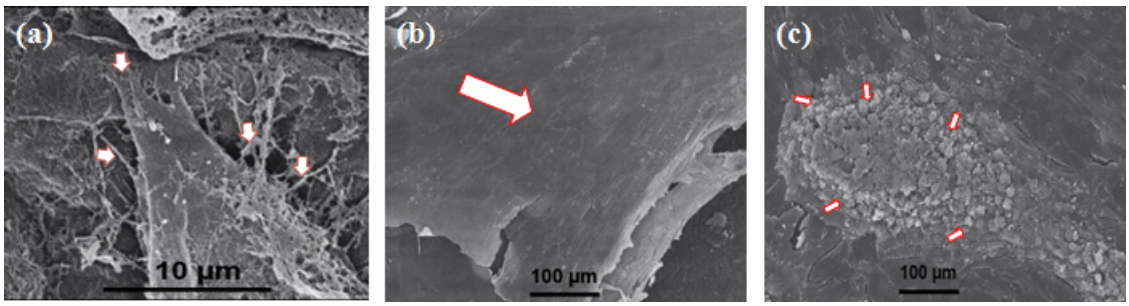

Figure 5. Primary rat cell morphology on SWNT matrix. (a) Representative SEM micrograph taken at day 3 showing cell attachment onto SWNTs on MCE substrate. Arrows indicate microfilaments. (b) Representative SEM micrograph taken at day 17 showing a confluent and differentiated cell layer during mid-stage formation of bone tissue (large arrow). (c) Representative SEM micrograph taken at day 23 showing characteristic late-stage calcification process (bone nodule-like formations, arrows).

In order to confirm that the increase in protein expression and the decrease in viable cell count at 24 h was due to cytotoxicity effects from loose nanotubes and not from well adhered nanotubes, we performed TEM analysis on cells grown on SWNTs on glass substrates because van der Waals interactions prevent the release of the latter. As mentioned previously, the SWNTs adhere very well to this substrate. This has been confirmed by TEM images shown in figures 6(g)–(h) corresponding to cell growth times of 24 and 72 h. The TEM images show that the number and concentration of inclusions in the cells grown on SWNTs on glass substrates are substantially lower.

Together, these data indicate that the uptake of nanotubes by the bone cells during the initial 24 h period on SWNTs on MCE substrates is responsible for the toxicity which leads to the decrease in cell count and final increase in ECM levels. While a detailed elucidation of the mechanisms of carbon nanotube uptake will require further investigation, our results are consistent with the work of Yehia *et al* which showed carbon nanotube uptake in HeLa cells [31]. However, the increase in protein expression on SWNT substrate is difficult to reconcile with toxicity results. We suggest the following: cells contain several growth factors in their cytoplasm. Nanotube uptake would cause cellular damage and subsequent release of growth factors such as FGF or TGF that may act to stimulate either the growth or differentiation of the surviving cells [32, 33]. In fact, Cui *et al* have shown that nanotube-mediated cytotoxicity is associated with increase in amount of proteins detected in the culture media [34]. Therefore to test the idea that the release of growth factors from the dying cells acts to boost the function of the surviving cells, we supplemented primary cells seeded on control substrate with a small amount of cell lysate after 3 and 24 h. This treatment was sufficient to boost the synthesis of protein so that at day 21 the levels were comparable to those on SWNTs on MCE substrates, as shown in figure 7.

Although the total amount of protein expressed in lysed cultures is lower, the overall trend is increased protein production which is comparable between the SWNTs on MCE and polystyrene samples to which lysate was supplemented, as indicated in figure 7. That is, the rate of protein production steeply increased after the second week of culture, indicating that the release of endogenous growth factors during the first days of culture had profound and long-lasting effects on histogenesis of bone formation.

4. Discussion

Our results offer some intriguing insight into biological applications of nanomaterials. For example, CNTs have been reported to be toxic to mammalian cells through increasing oxidative damage via activation of the nuclear transcription factor NF-κB and cause G1 phase arrest, apoptosis and impairment of cellular adhesion [16, 34]. In clinical trials with rodents, Lam *et al* found that CNTs induced inflammation, epithelioid granulomas, fibrosis, and biochemical/toxicological changes in the lungs [35]. On the other hand, a number of investigations have shown that CNTs can sustain cell growth (3T3-L1 mouse fibroblasts) and, in the case of bone cells (osteosarcoma ROS 17/2.8), support histogenesis [36, 3]. Clinical studies using mice reported that multi-walled CNTs adjoining bone accelerate bone formation and when anodized titanium, one of the most commonly used materials for bone implant was mixed with CNTs, osteoblast functions were significantly enhanced [37]. Our findings show that both views are essentially correct. In fact, carbon nanotubes are toxic to the cells, when adsorbed by a process resembling phagocytosis. However when uptake of CNTs, and thus the number of killed cells, remains limited, it promotes the release of growth factors (by the dead cells) that act to stimulate in the long-range, post-mitosis processes such as synthesis of extracellular matrix, thereby enhancing bone tissue histogenesis.

Osteoblast primary cell cultures are known to include not only osteoblast cells, which are predominant, but also some residual number of macrophages and fibroblasts. Chang *et al* studied the effect of resident macrophages on osteoblast cell function and found that the cells played an important role in bone homeostasis [38]. Future tests should carefully investigate effect of SWNTs on specific cell lines to determine which cell type predominantly internalize nanotubes, undergo apoptosis and contribute to bone histogenesis.

A crucial difference between our work and other reports in the literature is a fact that we observed a toxicity induced cell response that is controlled by loose nanotubes in cell

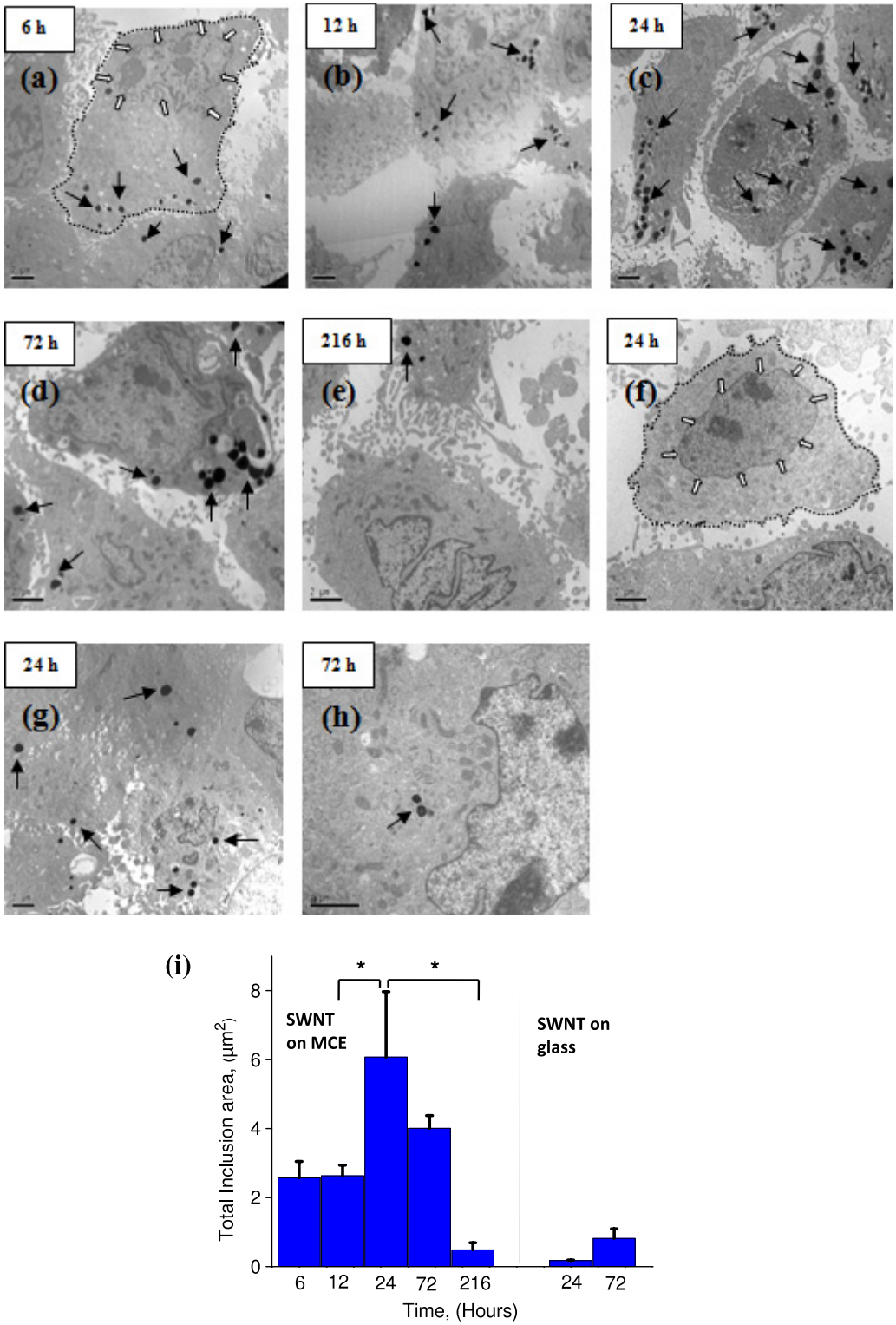

Figure 6. TEM images of sectioned cells with carbon nanotube inclusions. ((a)–(e)) MC3T3-E1 cells grown on SWNTs on MCE substrate were collected at various time points to monitor carbon nanotube uptake. In (a) the plasma membrane is underlined by a dotted line. The white arrows indicate the nucleus. Black arrows indicate carbon content within the cell cytoplasm. (f) Control on polystyrene at 24 h. Black arrows, dotted line and white arrows as in (a). ((g)–(h)) SWNTs on glass at 24 and 72 h. Scale bars are 2 μm. (i) Total carbonaceous areas of SWNT inclusions at the indicated time points on the indicated substrates. Values are the mean $\pm$ SEM of six micrographs. Statistical differences are indicated with $*$; $p < 0.05$.

cultures. However, in order to observe toxicity-mediated cell growth, a minimum number of cells is required. We found that if the primary cell number is very low ($\sim$5500 cm^{-2}) then the SWNT uptake leads to the death of the entire cell population. A typical number of primary cells used to observe toxic effect and subsequent cell recovery was at 9000 cm^{-2}.

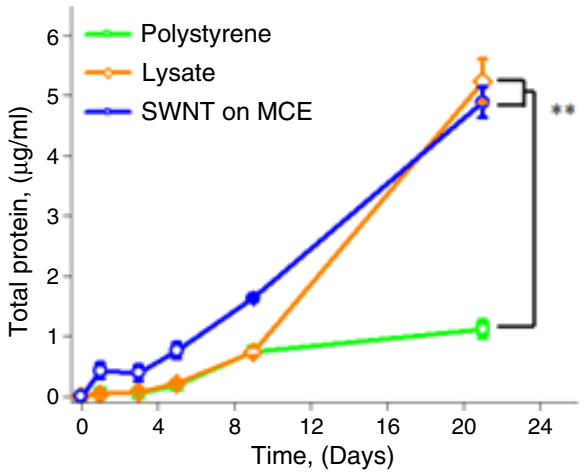

Figure 7. Release of cytosol improves cell growth. Total protein at different time points for cells grown on SWNTs on MCE (circles), polystyrene (squares) and on polystyrene supplemented with lysates of primary calvariae osteoblastic cells (diamonds). Values are mean ± SD of three independent cell cultures. Statistically significant differences from control are indicated with $**$; $p < 0.01$.

This effect cannot be observed when using a high initial number of cells [37]. Thus, our results suggest that the effect of SWNT/cellular interactions are not only influenced by the biological environment but can also influence the biochemistry of the local environment.

5. Conclusions

In summary, we have demonstrated that osteoblast cells grown onto SWNTs on multicellulose ester (MCE) substrates experienced some toxicity from uptake of loose SWNTs. At sufficient dosage of SWNTs after 24 h, cell death was observed. Cell destruction leads to release of proteins and other factors that stimulate remaining cells causing them to produce higher levels of the osteoblast phenotype markers such as Collagen I and alkaline phosphatase activity. We also performed control experiments with SWNTs on glass substrates where little or no uptake of SWNTs by cells occurred due to the absence of loose nanotubes. The cell activity on SWNTs on glass substrates was comparable to reference substrates. Finally, to test whether the enhanced protein expression for SWNTs on MCE was due to growth factors released by burst cells, we performed another control experiment in which lysed cells were added to cell cultures on reference substrates. This was done to mimic the introduction of growth factors by cell death on SWNTs on MCE substrates. The results showed that the introduction of lysed cells has the same impact on extracellular matrix expression. Thus, our observations can reconcile the apparent toxicity and benefits of SWNT substrates for osteoblast cell proliferation and differentiation.

References

[1] Hu H, Ni Y, Montana V, Haddon R C and Parpura V 2004 *Nano Lett.* **4** 507–11
[2] Kalbacova M, Kalbac M, Dunsch L, Kataura H and Hempel U 2006 *Phys. Status Solidi* b **13** 243
[3] Zanello L P, Zhao B, Hu H and Haddon R C 2006 *Nano Lett.* **6** 562–7
[4] Rinkevich B, Ben-Yakir S and Ben-Yakir R 1999 *Biol. Bull.* **197** 11–3
[5] Schroeder A, Francz G, Bruinink A, Hauert R, Mayer J and Wintermantel E 2000 *Biomaterials* **21** 449–56
[6] Ignjatovic N, Tomic S, Dakic M, Miljkovic M, Plavsic M and Uskokovic D 1999 *Biomaterials* **20** 809–16
[7] Correa-Duarte M A, Wagner N, Rojas-Chapana J, Morsczeck C, Thie M and Giersig M 2004 *Nano Lett.* **4** 2233–6
[8] Schwartz Z, Lohmann C H, Sisk M, Cochran D L, Sylvia V L, Simpson J, Dean D D and Boyan B D 2001 *Biomaterials* **22** 731–41
[9] Nishimura I, Huang Y, Butz F, Ogawa T, Lin A and Wang C J 2007 *Nanotechnology* **18** 245101
[10] Yu M F, Files B S, Arepalli S and Ruoff R S 2000 *Phys. Rev. Lett.* **84** 5552
[11] Dalton A B, Collins S, Munoz E, Raza J M, Ebron V H, Ferraris J P, Coleman J N, Kim B G and Baughman R H 2003 *Nature* **423** 703
[12] Baugman R H *et al* 1990 *Science* **284** 1340–4
[13] Kagan V E *et al* 2006 *Toxicol. Lett.* **165** 88–10
[14] Usui Y *et al* 2008 *Small* **4** 240–6
[15] Zhang D, Yi C, Zhang J, Chen Y, Yao X and Yang M 2007 *Nanotechnology* **18** 475102
[16] Manna S K, Sarkar S, Barr J, Wise K, Barrera E V, Jejelowo O, Rice-Ficht A C and Ramesh G T 2005 *Nano Lett.* **9** 1676–84
[17] Chiang I W, Brinson B E, Huang A Y, Willis P A, Bronikowski M J, Margrave J L, Smalley E and Hauge R H 2001 *J. Phys. Chem.* B **105** 8297–301
[18] Xu Y Q, Peng H, Hauge R H and Smalley R E 2005 *Nano Lett.* **5** 163–8
[19] Unalan H E 2006 *PhD Thesis* Rutgers, The State University
[20] Wu Z *et al* 2004 *Science* **305** 1273–6
[21] Fanchin G, Unalan H E and Chhowalla M 2006 *Appl. Phys. Lett.* **88** 191919
[22] Unalan H E, Fanchini G, Kanwal A, Pasquier A D and Chhowalla M 2006 *Nano Lett.* **6** 677–82
[23] Shalhoub V, Conlon D, Tassinari M, Quinn C, Partridge N, Stein G S and Lian J B 1992 *J. Cell Biochem.* **50** 425–40
[24] Kwok S, Qin L, Partridge N C and Selvamurugan N 2005 *J. Cell Biochem.* **95** 1002–11
[25] Bradford M 1976 *Anal. Biochem.* **72** 248–54
[26] Bornstain M B 1958 *Lab. Investig.* **7** 134–7
[27] Millan J L 2006 *Mammalian Alkaline Phosphatases* ed A G Marangoni, H Bisswanger, R A Copeland and C H Suelter (Weinheim: Wiley–VCH) pp 108–48
[28] Gerstenfeld L C, Chipman S D, Glowacki J and Lian J B 1978 *Dev. Biol.* **122** 49–60
[29] Shi Kam N W, Jessop T C, Wender P A and Dai H 2004 *J. Am. Chem. Soc.* **126** 6850–1
[30] Porter A E, Gass M, Muller K, Skepper J N, Midgley P A and Welland M 2007 *Nat. Nanotechnol.* **2** 713–7
[31] Yehia H N, Draper R K, Mikoryak C, Walker E K, Bajaj P, Musselman I H, Daigrepont M C, Dieckmann G R and Pantano P 2007 *J. Nanobiotechnol.* **5** 8
[32] Clarke M S and Feeback D L 1996 *FASEB J.* **10** 508
[33] Roberts A B *et al* 1986 *Biochemistry* **83** 4167–71
[34] Cui D, Tian F, Ozkan C S, Wang M and Gao H 2005 *Toxicol. Lett.* **155** 73–85
[35] Lam C W, James J T, McClusky R, Arepalli S and Hunter R L 2006 *Crit. Rev. Toxicol.* **36** 189–217
[36] Meng J, Song L, Meng J, Kong H, Zhu G, Wang C, Xu L, Xie S and Xu H 2006 *J. Biomed. Mater. Res.* A **10** 298–306
[37] Sirivisoot S, Yao C, Xiao X, Sheldon B and Webster T J 2007 *Nanotechnology* **18** 365102
[38] Chang M K, Raggatt L, Alexander K A, Kuliwaba J S, Fazzalari N L, Schroder K, Maylin E R, Ripoll V M, Hume D A and Pettit A R 2008 *J. Immunol.* **18** 1232–44